Kinetics and Catalysis, Vol. 42, No. 6, 2001, pp. 857–866. Translated from Kinetika i Kataliz, Vol. 42, No. 6, 2001, pp. 938–947.

Physicochemical Properties of Mesoporous Mesophase Silicate Materials Formed via the Electrostatic S^+I^- Mechanism[1]

V. N. Romannikov*†, S. D. Kirik, L. A. Solov'ev**, A. N. Shmakov*, A. Yu. Derevyankin*, V. B. Fenelonov*, O. A. Kholdeeva*, O. B. Lapina*, and E. A. Paukshtis***

** Boreskov Institute of Catalysis, Siberian Division, Russian Academy of Sciences, Novosibirsk, 630090 Russia*

*** Institute of Chemistry and Chemical Technology, Siberian Division, Russian Academy of Sciences, Krasnoyarsk, 660049 Russia*

Received July 20, 2000

Abstract—The formation of the structure of a highly organized silicate mesoporous mesophase material (MMM) with hexagonal packing via the S^+I^- reaction pathway and MMM-based aluminosilicates (Al,Si)-MMM and titanosilicates (Ti,Si)-MMM with different concentrations of the elements are considered. The structural, textural, and catalytic properties of the materials are studied.

INTRODUCTION

This work continues our earlier studies [1–4] of the formation and physicochemical properties of silicate mesoporous mesophase materials (MMMs). These materials have been known since the early 1990s [5]. These are highly organized systems whose structure is formed with the participation of inorganic components (I) and surfactants (S). The pore space formed in these materials after surfactant removal is highly organized and is formed by mesopores of a standardized size in a nanometer scale. The mesopore surface area in MMMs is ~1000 m^2/g and the mesopore volume is ~1 cm^3/g. As the chemical composition of an inorganic wall in MMMs can be varied in a wide range, MMMs are of great interest for the development of new catalytic systems, particularly, for the low-temperature transformations of large molecules.

The key point of structure formation is the type of the interaction between the inorganic component and the surfactant. The following types of interactions are known: direct electrostatic (S^+I^- or S^-I^+) or indirect electrostatic ($S^+A^-I^+$ or $S^-K^+I^-$, where A^- or K^+ is an additional anion or cation, respectively) interactions [6], the formation of a hydrogen bond (S^0I^0) [7], and the formation of a covalent bond (S^0–I^0) [8].

This study was aimed at the optimization of the conditions of the formation of highly organized SiO_2-MMM with the *p*6*mm* hexagonal packing through the S^+I^- reaction pathway; the preparation of MMM-based aluminosilicates (Al,Si)-MMM and titanosilicates (Ti,Si)-MMM with different concentrations of the elements; and the investigation of the structural, textural, and catalytic properties of the final materials.

† Deceased.

[1] Presented at the II All-Russian Workshop on Highly Organized Catalytic Systems (Moscow, June 27–30, 2000).

EXPERIMENTAL

Materials. The materials were synthesized according to a common procedure described in [3] by the hydrothermal treatment of reaction mixtures under static conditions (20–165°C, 40–50 h). The reaction mixtures had the following molar composition (pH 8–11):

$$(0.95\text{–}1.00)SiO_2 \cdot (0.05\text{–}0)EO_n$$
$$\cdot\, xC_{16}H_{33}N(CH_3)_3Br \cdot y\text{NaOH} \cdot 50H_2O,$$

where E = Al or Ti; x = S/(Si + E) was varied within the range 0.1–0.3; y = OH/(Si + E) was varied within the range 0.1–0.5. $C_{16}H_{33}N(CH_3)_3Br$ was used as the cationic surfactant (C_{16}-S). The surfactant cations were removed from the initial materials by oxidative thermal treatment at 550–600°C.

It follows from the preparation procedure that sodium cations are present in the reaction mixture in which a silicate mesostructure is formed. The concentration of sodium in the product (SiO_2 mesostructure) is at most 0.05 wt % Na_2O in all of the repeatedly studied cases (see [1]), whereas this concentration in the aluminosilicate mesostructures is one order of magnitude lower: no higher than 0.005 wt % Na_2O (see [11]).

Structural analysis. The structural analysis was performed on a high-resolution diffractometer at the Siberian Center of Synchrotron Radiation (Budker Institute of Nuclear Physics, Siberian Division, Russian Academy of Sciences, Novosibirsk). A Si(111) crystal monochromator provided the degree of monochromation $\Delta\lambda/\lambda \sim 10^{-4}$. The high natural collimation of the synchrotron radiation beam in the vertical plane made it possible to obtain a high spatial resolution of the diffractometer by mounting a flat perfect Ge(111) crystal analyzer on the diffracted beam. The instrumental broadening of the reflections in a 2θ angle range of 1°–7° was at most $\Delta(2\theta) \sim 0.04°$. To confine the azi-

0023-1584/01/4206-0857$25.00 © 2001 MAIK "Nauka / Interperiodica"

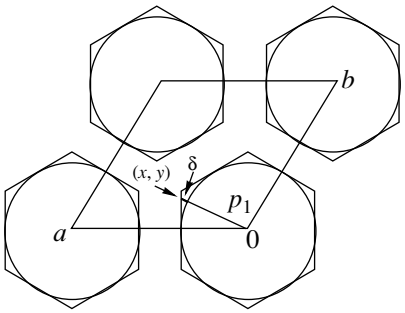

Fig. 1. Schematic diagram of structure model parameters.

muthal divergence of the diffracted beam and to lower the asymmetry of reflections toward small angles, a vertical parallel collimator (Soler collimator) with a divergence of 5 milliradians was used.

Textural analysis. The textural analysis of the systems was carried out by the combined structure–adsorption method described in [9]. According to this approach, the following relationships are fulfilled for a hexagonal (honeycomb) structure: $a_0 = d_{meso} + h_w$ and $d_{meso} = a_0(\varepsilon_{meso})^{1/2}$, where a_0 is the lattice parameter; d_{meso} is the effective mesopore diameter; h_w is the thickness of an inorganic wall; and ε_{meso} is the porosity determined from the specific volume of the mesopores V_{meso} and the true density ρ according to the equation $\varepsilon_{meso} = V_{meso}\rho/(1 + V_{meso}\rho)$. The specific volume of the mesopores was determined from nitrogen adsorption isotherms measured at 77 K according to a standard procedure on a Micromeritics ASAP-2400 instrument.

Simulation of the structure of materials. The structure of the materials was simulated based on a previously described approach [10] by the examination of the structure factors

$$F(hk) = \frac{1}{S_0}\int_{S_0}\rho(x, y)\exp(2\pi i(hx + ky))\mathrm{d}x\mathrm{d}y$$

by the Rietveld method in combination with the concept of continuous electron density

$$\rho(x, y) = \sum_{m=1}^{n} p_{4m}[1 + \tanh(p_{3m}(R(x, y) - p_{1m} - p_{2m}\delta(x, y)))],$$

which is described as the sum of n overlapped coaxial regions with varying shapes (from cylinder to hexagonal prism) and different densities (Fig. 1). Here, S_0 is the surface area of a two-dimensional cell; $R(x, y)$ is the distance of point (x, y) from the origin; p_1 is the radius of a cylinder inscribed in the mesopore; p_2 in combination with $\delta(x, y)$ are the parameters of the transformation of the cylinder to the hexagonal prism; p_3 is the parameter that describes the slope of the electron density of the wall; and parameter p_4 controls the cylinder density. The structure simulation was based on the concept from [10] that the mesostructure is the hexagonal packing of mesopores separated by an inorganic (silicate) wall. Obviously, this concept follows from the electron-microscope micrographs of these systems, which were previously reported in the literature.

The computation was performed using the modified Rietveld DBWS-90006PC program. The maps of the electron-density distribution were constructed with the use of integral intensities. A detailed description of the method was given in [10].

State of aluminum. The state of aluminum atoms was studied with the use of ^{27}Al MAS NMR spectra recorded on a Bruker MSL-400 spectrometer (ν_0 = 104.2 MHz) with magic angle spinning (12 kHz). Before measurements, all samples were saturated with water vapor. Chemical shifts were measured with reference to $Al(H_2O)_6^{3+}$ used as an external standard.

Saturation with water vapor was performed to determine the degree of aluminum cluster formation in the silicate wall because under these conditions mesopores are completely filled with water and unclustered (isolated) aluminum ions are not stabilized on the surface of the silicate wall (they occur in an aqueous solution). Therefore, the width of the NMR signal from these Al ions is very close to that observed for an Al aqua complex, for example, in an aqueous nitrate solution. An increase in the degree of cluster formation is accompanied by a decrease in the fraction of isolated Al as can be seen in the NMR spectra. Previously, the method was outlined in a special paper on aluminosilicates (see [11]).

State of titanium. The state of titanium atoms was studied using the IR spectra of adsorbed CO, which were recorded on a Bruker IFS-113v Fourier spectrometer, and UV diffuse-reflectance spectra.

Catalytic properties. The catalytic properties of aluminosilicates were studied in gas-phase benzene alkylation with isobutene in a flow reactor at an atmospheric pressure. The reaction conditions were as follows: the initial benzene/isobutene molar ratio was 10, the weight feed rate was 1.1–1.3 h^{-1}, and the temperature of the catalyst bed was 150 ± 3°C.

The catalytic properties of titanosilicates were studied in the liquid-phase oxidation of alkenes and thioethers with H_2O_2 at temperatures of 50 and 20°C, respectively, in an acetonitrile medium. The procedures were described in more detail in [11, 12].

RESULTS AND DISCUSSION

According to the electron-microscopic images of MMMs [1, 5], the structure of C_{16}-SiO_2-MMM can be presented as the hexagonal packing of cylindrical or hexagonal mesopores. When this structure is highly organized and the mesopores have exactly the same

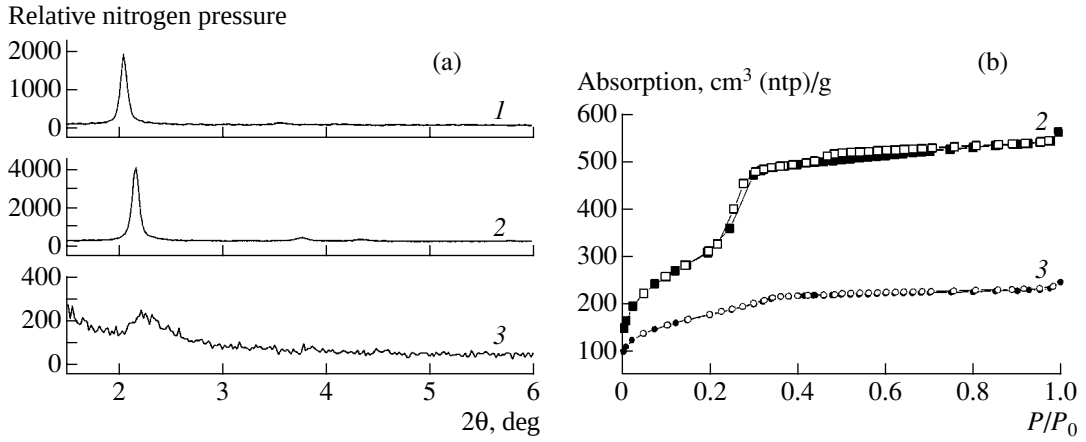

Fig. 2. (a) X-ray diffractograms and (b) nitrogen adsorption isotherms for C_{16}-SiO_2-MMM: (*1*) initial sample containing surfactant cations, (*2*) calcined sample, and (*3*) hydrated and repeatedly calcined sample.

diameter, which is constant along the mesopore, such a hexagonal packing should be considered as ideal.

In this case [3]: (1) The high organization of the MMM structure implies that its lattice parameter a_0 is constant. In turn, this suggests that reflections in the X-ray diffractograms of mesophase systems should be narrow (with a half-width close to the experimental error). (2) The absence of a spread in diameter for different mesopores indicates that the $\Delta(P/P_0)$ region within which the capillary condensation of nitrogen takes place during adsorption is very narrow. (3) The strictly constant diameters of all mesopores along their lengths imply that the adsorption and desorption branches of the nitrogen adsorption isotherm of this system strictly coincide at least for a pore size of 4.5 nm or smaller.

As a result of the optimization of the formation conditions [3], we found that highly homogeneous initial mixtures should be used, and the optimal parameters of the synthesis are $x = S/(Si + E) = y = OH/(Si + E) \approx 0.2$, which correspond to pH 8.0–8.5. The characteristics of the initial and calcined C_{16}-SiO_2-MMM forms obtained under these conditions are in complete agreement with the above notion of the properties of an ideal structure (Fig. 2, curves *1*, *2*). At the same time, the hydration of a calcined sample followed by repeated calcination (Fig. 2, curves *3*) resulted in almost complete degradation of the C_{16}-SiO_2-MMM structure. Hence, this structure is unstable to water, which is likely due to the structure of the silicate wall.

Figure 3 illustrates the simulated structures of MMMs of silicate and aluminosilicate chemical composition as the maps of electron density distribution. It can be seen that, in both materials, the shape of mesopores is much closer to a hexagonal prism than to a cylinder. The reliability of the results obtained was discussed in detail in [10]. It was found [10] that the introduction of the p_{21} parameter, which characterizes the hexagonal character of mesopores, significantly improves the agreement between experimental and calculated X-ray diffraction patterns. Thus, in the calculation of the electron-density map for C_{16}-SiO_2-MMM, the R_F factor, which characterizes the discrepancy between the experimental and simulated X-ray diffractograms, was equal to 9.45% at $p_{21} = 0$ (cylindrical pore) or 2.14% at $p_{21} = 0.62$ (partially hexagonal pore).

In both cases, the removal of surfactant cations by the oxidative thermal treatment of the initial MMM forms resulted, as expected, in a sharp decrease of the electron density in the mesopore volume. Simultaneously, it can be seen in the maps (Figs. 3a, 3b) that the electron density in the wall of C_{16}-SiO_2-MMM is not constant: a maximum is observed at the junction points of three neighboring prisms and a minimum, in the line connecting the centers of neighboring prisms. The whole structure can be described as consisting of blocks separated by zones with a lowered electron density (conditionally, "gaps"). It is likely that this is the reason for the above structural degradation of C_{16}-SiO_2-MMM on the calcination of the material when the mesopores were filled with water. At the same time, in the case of the C_{16}-(Al,Si)-MMM system with the atomic ratio $Al/(Al + Si) = 0.05$ (Figs. 3c, 3d), an electron-density maximum (for the initial form) rather than a minimum as in the case of C_{16}-SiO_2-MMM was observed in the line connecting the centers of neighboring mesopores; a nearly constant electron density at the wall was observed in the calcined form. Such features of the wall structure in the aluminosilicate MMMs are likely due to the filling of defects inside the purely silicate wall with aluminum ions.

Indeed, as the aluminum concentration in the C_{16}-(Al,Si)-MMM test samples was increased, their structure remained highly organized in both the initial and calcined samples is retained: FWHM of the (100) reflection was no higher than 2θ 0.07° (Figs. 4a, 4b; Fig. 5, curve *3*) and the effective wall thickness h_w remained almost constant in the whole range of the

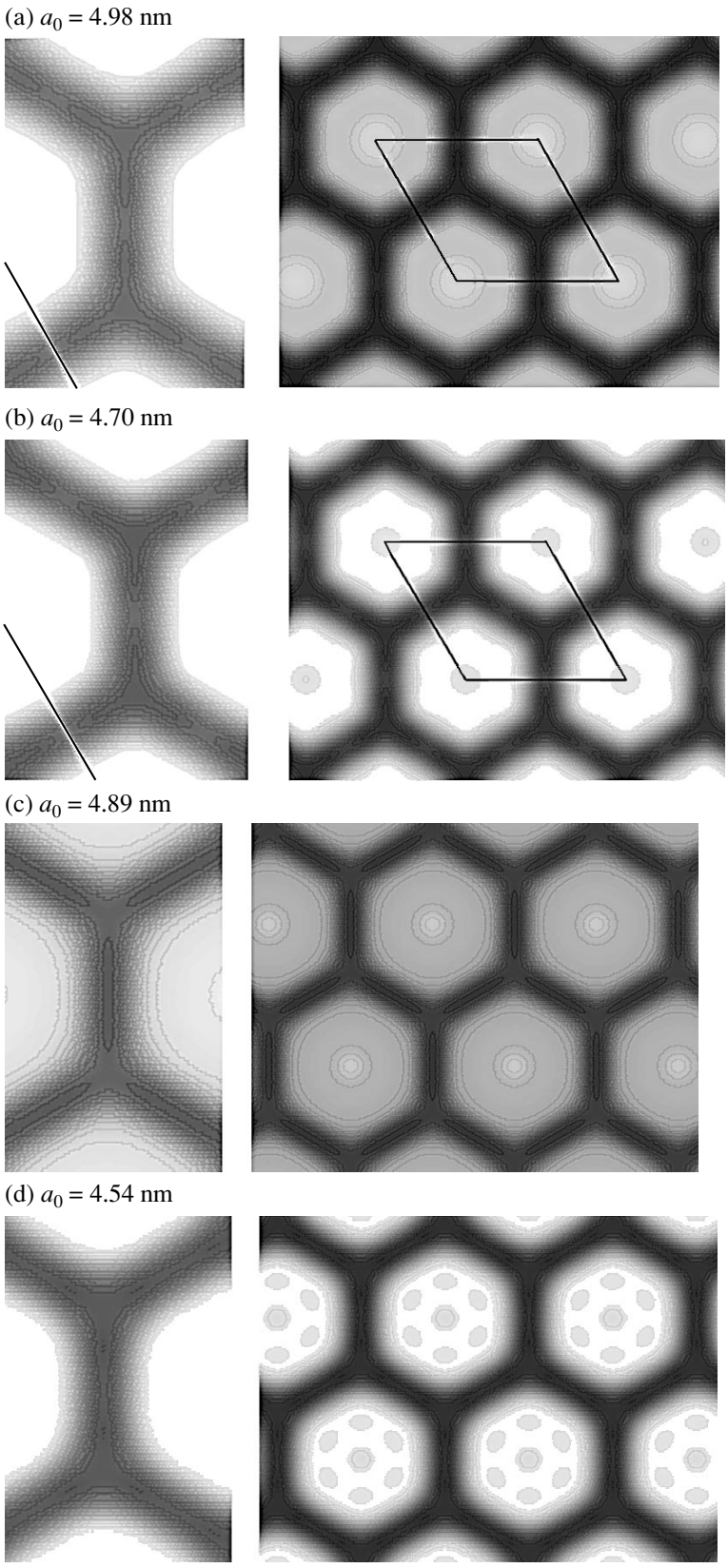

Fig. 3. Maps of electron-density distribution for C_{16}-SiO_2-MMM and C_{16}-(Al,Si)-MMM with the atomic ratio Al/(Al + Si) = 0.05: (a) initial C_{16}-SiO_2-MMM sample, (b) calcined C_{16}-SiO_2-MMM sample, (c) initial C_{16}-(Al,Si)-MMM sample, and (d) calcined C_{16}-(Al,Si)-MMM sample. Magnified fragments show the electron-density distribution in inorganic walls in detail.

compositions (Fig. 5, curve *6*). Significant changes in the structure of these materials occurred upon the calcination of hydrated samples. The lower the total aluminum concentration in the samples; that is, the closer their composition to that of pure C_{16}-SiO_2-MMM, the greater a decrease in the intensity of the (100) reflection (Fig. 4c) and an increase in its FWHM (Fig. 5, curve *4*). At the same time, almost no structural changes occurred upon the calcination of hydrated C_{16}-(Al,Si)-MMM at relatively high aluminum concentrations (Al/(Al + Si) ≥ 0.03–0.04), and this fact agrees completely with the electron-density distribution in their walls (Figs. 3c, 3d).

The results of studying the state of aluminum atoms in C_{16}-(Al,Si)-MMM are presented in Fig. 6 (^{27}Al MAS NMR spectra) and in Table 1 (the main parameters of the spectra). As can be seen, an increase in the Al concentration in C_{16}-(Si,Al)-MMM results in two main changes in the spectra. First, the integral intensity of the ^{27}Al MAS NMR spectra of calcined samples decreases compared to the initial samples. Second, the signal from Al in an octahedral coordination (this signal can be detected in the samples after calcination) becomes broadened and finally disappears. Both facts suggest that the fraction of the state of aluminum in which the second coordination sphere of an aluminum atom also contains aluminum atoms increases with increasing aluminum content; that is, the fraction of aluminum atoms in the state of aluminum–oxide clusters increases. Taking into account the electron-density distribution in the wall of C_{16}-(Si,Al)-MMM (Figs. 3c, 3d) and the almost constant structure and texture parameters in the initial and calcined forms of this system, it is believed that such aluminum–oxide clusters are formed in the gaps of purely silicate C_{16}-SiO_2-MMM (Figs. 3a, 3b).

Note that the broadening of peaks at 0.8 ppm is likely due to the insufficiently correct subtraction of the background spectrum of a rotor in which the test sample was placed for recording the spectrum. Unfortunately, this procedure is not always simple, and it cannot always be performed with an ideal accuracy. However, it is our opinion that the above imperfection of the spectrum has no effect on the interpretation of the physicochemical properties of mesostructured silicate materials.

The above structural peculiarities of C_{16}-(Si,Al)-MMM are in good agreement with the data on their catalytic activity (Table 2). It is seen that the activity of the samples slightly increases with aluminum concentration; however, it remains ~5–6 times lower than the activity of wide-pore zeolite Beta.

We decided on zeolite Beta as a reference sample for the reasons given below. The reference sample to be compared with the test systems should have the following properties: (1) it should be a heterogeneous acid–base catalyst; (2) a very high concentration of acid sites should be attainable; (3) the pore system of such a material should be maximally open (have a maximal size of input windows) in order to avoid the diffusional retardation of the acid–base transformations of monoaromatic hydrocarbons during their alkylation at

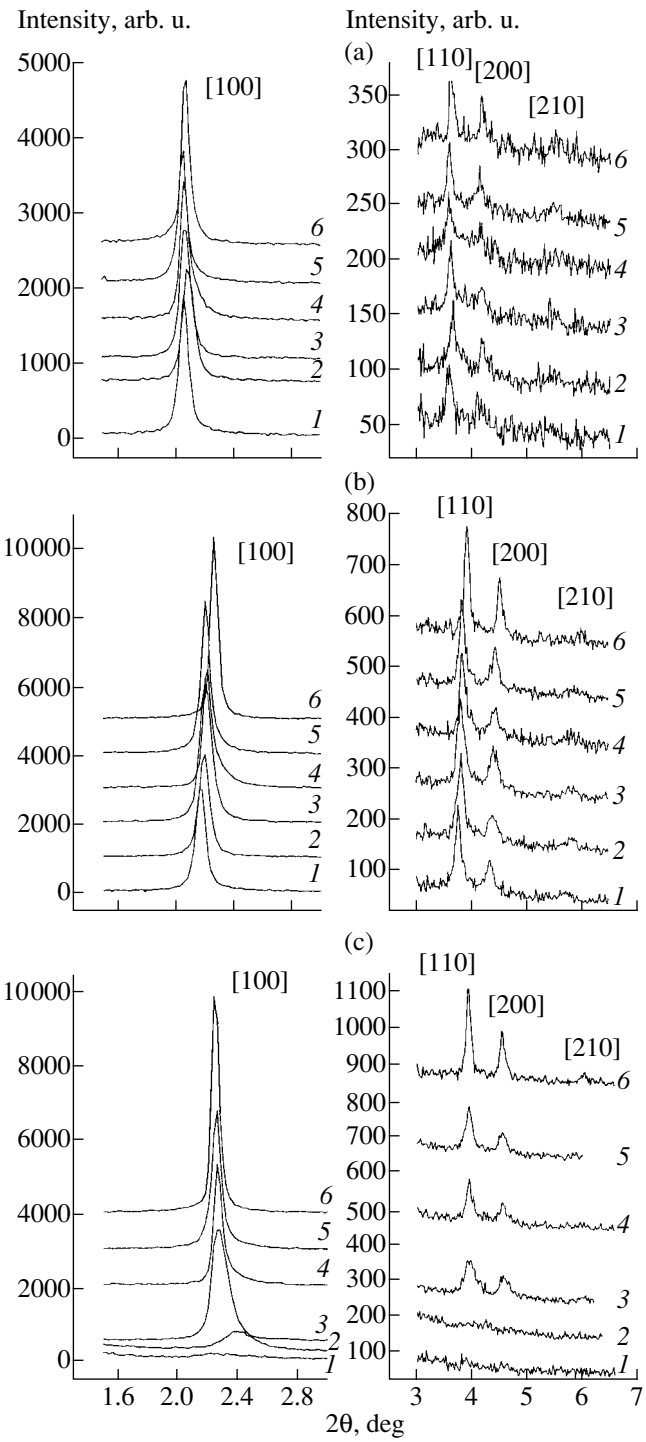

Fig. 4. X-ray diffractograms for C_{16}-(Al,Si)-MMM in (a) initial, (b) calcined, and (c) hydrated and repeatedly calcined forms. The Al/(Al + Si) atomic ratios are (*1*) 0, (*2*) 0.008, (*3*) 0.02, (*4*) 0.03, (*5*) 0.04, and (*6*) 0.05.

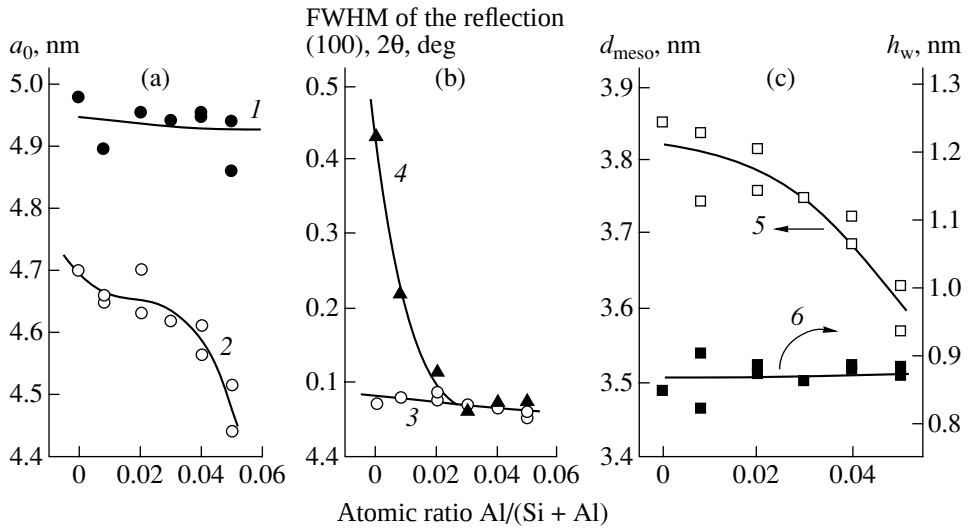

Fig. 5. (*1*, *2*) Lattice parameter a_0, (*3*, *4*) FWHM of the (100) reflection, (*5*) mesopore diameter d_{meso}, and (*6*) wall thickness h_w as functions of Al/(Al + Si) atomic ratio in the C_{16}-(Al,Si)-MMM systems for (*1*) initial, (*2*, *3*, *5*, *6*) calcined, and (*4*) hydrated samples.

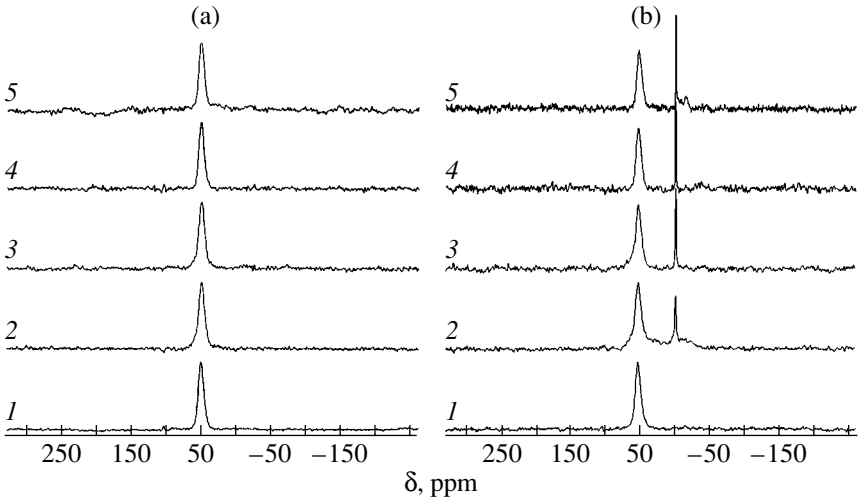

Fig. 6. ^{27}Al MAS NMR spectra of (a) initial and (b) calcined C_{16}-(Al,Si)-MMM samples. The Al/(Al + Si) atomic ratio is (*1*) 0.05, (*2*) 0.04, (*3*) 0.03, (*4*) 0.02, or (*5*) 0.008.

low reaction temperatures; and (4) the catalyst should be stable in operation (without deactivation by coke deposits) for a reasonably long time under the above conditions. Zeolite Beta is presently almost the only system that satisfies all of the four requirements simultaneously.

The possible reason for weak catalytic activity is the absence of considerable concentrations of strong acid sites from the test mesophase aluminosilicates. This fact is in good agreement with published data on the acidity and activity of aluminosilicate MMMs [14], and it is likely due to the formation of the above aluminum–oxide clusters. Indeed, such clustered aluminum atoms should have lowered acceptor ability toward the oxygen atom of the silanol OH group; therefore, they cannot participate in the formation of strong acid sites like bridging OH groups.

Similar structure peculiarities were also found for C_{16}(Ti,Si)-MMM titanosilicates, which also have a highly organized structure (Table 3). As can be seen in Fig. 7, the diffuse-reflectance UV spectra of samples 4 and 5 are similar (λ_{max} = 225 nm), and they suggest the isolated state of titanium ions [15]. As the titanium concentration increases (samples 1–3), the absorption maximum shifts to longer wavelengths and the absorption band broadens. This fact is likely indicative of the presence of partially clustered titanium–oxide species. This conclusion was also supported by IR-spectro-

Table 1. Main parameters of the ^{27}Al MAS NMR spectra of C_{16}-(Si,Al)-MMM samples

Atomic ratio Al/(Si + Al)	Initial samples				$\frac{I^{e}_{init}}{I_{cal}}$, %	Calcined samples			
	Al_t^a		Al_o^b			Al_t^a		Al_o^b	
	$\Delta\nu^c$, Hz	I^d_{rel}, %	$\Delta\nu^c$, Hz	I^d_{rel}, %		$\Delta\nu^c$, Hz	I^d_{rel}, %	$\Delta\nu^c$, Hz	I^d_{rel}, %
0.008	960	100	–	0	89	865	74	77	26
0.02	1010	100	–	0	82	894	77	183	23
0.03	1076	100	–	0	75	1068	80	212	20
0.04	1017	100	–	0	60	1033	84	250	16
0.05	1011	100	–	0	58	951	100	–	0

[a] Signal with the chemical shift δ_t = 51.8–53.4 ppm from aluminum in a tetrahedral coordination.
[b] Signal with the chemical shift δ_o = 0.8–0.9 ppm from aluminum in a octahedral coordination.
[c] Width of the NMR signal.
[d] Intensity of the NMR signal normalized to a weight unit of each sample separately.
[e] Integral intensity of the ^{27}Al MAS NMR spectrum observed for calcined samples relatively to initial samples.

Table 2. Catalytic properties of calcined C_{16}-(Si,Al)-MMM samples in benzene alkylation with isobutene. Zeolite Beta[a] was studied as a reference sample

Atomic ratio Al/(Si + Al)	Conversion, %		Selectivity, mol %, referred to converted benzene		Selectivity, mol %, referred to converted isobutene		
	benzene	isobutene[b]	*tert*-butylbenzene[b]	C_{11}^+ aromatic	*tert*-butylbenzene[b]	C_{11}^+ aromatic	C_5–C_{12} olefins
C_{16}-(Si,Al)-MMM							
0.008	0.5	32.4	80	20	12	4	84
0.02	1.2	37.9	74	26	21	10	69
0.03	1.2	39.3	74	26	21	14	65
0.04	1.3	42.2	70	30	25	13	61
0.05	1.4	43.3	66	34	21	17	62
Zeolite Beta							
0.048	7.1	76.7	88	10	82	13	3

[a] Zeolite-1 described in [13] with the concentration of strong proton sites (ν_{OH} = 3610 cm^{-1}) equal to 94 μmol/g.
[b] Selectivity for isobutylbenzene was much lower than 1 mol % for (Si,Al)-MMM samples and equal to ~1 mol % for zeolite Beta.

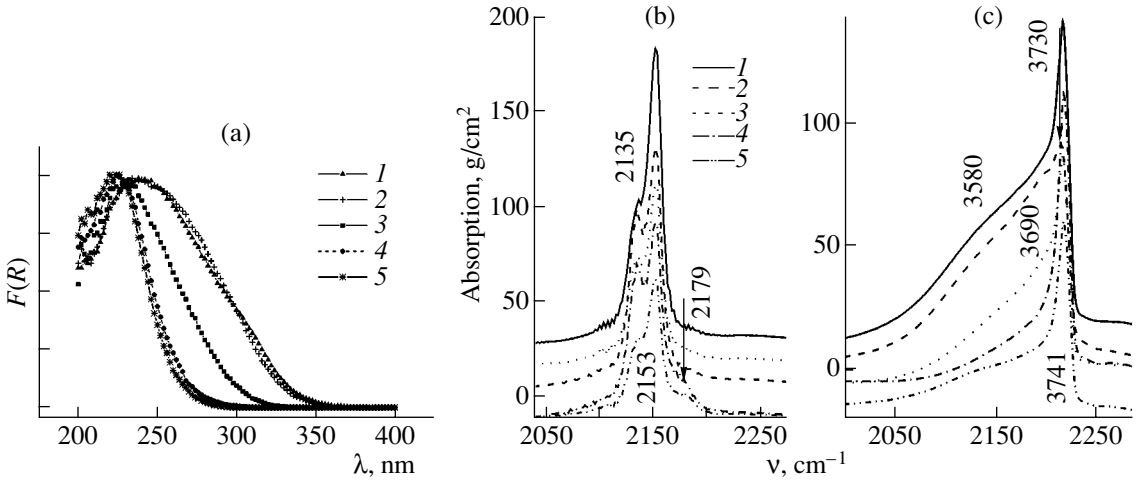

Fig. 7. (a) Diffuse-reflectance UV spectra and the IR spectra of (b) adsorbed CO and (c) the region of OH groups for calcined C_{16}-(Ti,Si)-MMM samples. The curve numbers correspond to the sample numbers in Table 3.

scopic data. Indeed, the spectra of adsorbed CO exhibit three bands: at 2135 cm^{-1} (corresponds to physically adsorbed CO), at 2153 cm^{-1} (corresponds to CO complexes with silanol groups observed at 3730–3740 cm^{-1} in the region of OH groups), and at 2179 cm^{-1} (corresponds to CO complexes with titanium cations localized outside the silicate matrix). The complexes of the last type are easily observable only in samples 1 and 2, which exhibited the highest concentrations of titanium (Table 3).

A study of the catalytic properties of C_{16}-(Ti,Si)-MMM showed that samples 3 and 4 with medium Ti concentrations were most active in cyclohexene oxidation (Table 4). In this case, both an increase and a decrease in the Ti concentration resulted in a decrease in the activity of C_{16}-(Ti,Si)-MMM. All of the C_{16}-(Ti,Si)-MMM test systems exhibited similar activities and selectivities toward thioether oxidation with hydrogen peroxide (Table 5). However, the activity of C_{16}-(Ti,Si)-MMM decreased in repeated tests after oxi-

Table 3. Structural and textural characteristics of calcined C_{16}-(Ti,Si)-MMM samples (2–5) and a Ti-HMS reference sample (1)

Sample	Atomic ratio Si/Ti	Structural parameters		Textural and adsorption properties			
		a_0[a], nm	FWHM[b], deg 2θ	S_{meso}[c], m^2/g	S_{ext}[d], m^2/g	V_{meso}[e], cm^3/g	$\Delta(P/P_0)$[f]
1	30	–	> 0.5	627	170	0.887	0.327
2	19	4.47	0.117	911	86	0.738	0.071
3	49	4.64	0.078	1059	53	0.908	0.064
4	124	4.68	0.086	1068	48	0.932	0.062
5	166	4.71	0.093	1015	44	0.887	0.064
6[g]	∞	4.72	0.071	1065	44	0.930	0.067

[a] Lattice parameter.
[b] Half-width of reflection [100].
[c] Surface area of mesopores.
[d] External surface area of particles.
[e] Mesopore volume.
[f] Pressure range of nitrogen capillary condensation.
[g] Sample corresponds to C_{16}-SiO_2-MMM.

Table 4. Catalytic properties of calcined C_{16}-(Ti,Si)-MMM in liquid-phase cyclohexene oxidation with H_2O_2. The sample numbers correspond to those in Table 3

Sample	Cyclohexene conversion for 4 h, %	Selectivity to epoxide[a], %	Yield of the products of cyclohexene oxidation[b], %	Conversion of H_2O_2 for 4 h, %	Decomposition[c] of H_2O_2 for 4 h, %
1	28	32	49	57	30
2	28	18	45	55	48
3	33	18	41	73	52
4	31	19	36	79	46
5	18	33	23	70	67

[a] On a converted cyclohexene basis.
[b] On a converted H_2O_2 basis.
[c] In the absence of cyclohexene.

Table 5. Catalytic properties of calcined C_{16}-(Ti,Si)-MMM in liquid-phase methyl phenyl sulfide (MPS) oxidation with H_2O_2

Testing cycle	Ti, wt %	MPS conversion in 20 min, %	Product distribution, %	
			sulfoxide	sulfone
Before reaction	0.58	–	–	–
I cycle	0.61	95	76	24
II cycle	0.57	84	77	23
III cycle	0.62	74	76	24

dative thermal treatment. The decrease in activity cannot be due to the washout of titanium from the catalyst because the titanium concentration did not decrease in this case (Table 5). It is most probable that the observed changes in the catalytic properties are caused by the structural degradation of C_{16}-(Ti,Si)-MMM.

CONCLUSION

The formation of a silicate MMM via the S^+I^- reaction pathway in weakly alkaline media suggests the electrostatic interaction of surfactant cations with polysilicate anions. Hence, the composition of the initial MMM species can be described schematically as the alkyltrimethylammonium polysilicate $\{C_nH_{2n+1}N(CH_3)_3^+\}\{^-O[Si(OH)_2O]_mSi(OH_3\}$, where $(m + 1) \approx (1/\alpha)$, and $\alpha = (N/Si) \approx 0.2$. This formula suggests that at least a fraction of oxygen atoms of the inorganic part (wall) of the material has a negative charge, providing the interaction with the surfactant cation. Unlike the electrically neutral SiOH groups, these charged oxygen atoms cannot form the siloxane groups Si–O–Si by condensation during hydrothermal treatment. It is likely that they are responsible for the appearance of gaps (a decrease in electron density) in the silicate walls to result in the block structure of the system.

It is known that to develop active acid–base or redox catalytic systems on the basis of silicate MMMs, isolated Al or Ti atoms in a tetrahedral coordination with oxygen atoms are required. This situation is most easily achieved in dilute systems. However, when the Al or Ti concentration is relatively small, the structure of a silicate MMM exhibits a low resistance to water. The problem of the stability to water can be solved by an increase in the Al (or Ti) concentration in the MMM. However, element–oxide clusters are formed in this case, and the catalytic activity of the MMM is low.

It seems that this problem can be solved by a change in the type of interaction between a surfactant and an inorganic component that participate in the MMM formation. Such approaches are being studied intensively.

ACKNOWLEDGMENTS

This work was supported by the Russian Foundation for Basic Research (project no. 98-03-32390), International Science Foundation (grant no. IR-97-0676), the Russian Academy of Sciences, Program for Young Scientists, 1999 (grant no. 156), and the Ministry of Education of the Russian Federation (grant no. 98-8-5.2-50).

REFERENCES

1. Romannikov, V.N., Fenelonov, V.B., Nosov, A.V., *et al.*, *Izv. Akad. Nauk, Ser. Khim.*, 1999, vol. 10, p. 1845.
2. Romannikov, V.N., Fenelonov, V.B., and Derevyankin, A.Yu., *Izv. Akad. Nauk, Ser. Khim.*, 1999, vol. 10, p. 1852.
3. Kodenev, E.G., Shmakov, A.N., Derevyankin, A.Yu., *et al.*, *Izv. Akad. Nauk, Ser. Khim.*, 2000, vol. 10, p. 1685.

4. Romannikov, V.N., Fenelonov, V.B., Nosov, A.V., *et al.*, *Kinet. Katal.*, 2000, vol. 41, no. 1, p. 108.
5. Kresge, C.T., Leonowicz, M.E., Roth, W.J., *et al.*, *Nature*, 1992, vol. 359, p. 710; Beck, J.S., Vartuli, J.C., Roth, W.J., *et al.*, *J. Am. Chem. Soc.*, 1992, vol. 114, p. 10834.
6. Huo, Q., Margolese, D.I., Ciesla, U., *et al.*, *Nature*, 1994, vol. 368, p. 317.
7. Bagshaw, S.A., Prouzet, E., and Pinnavaia, T.J., *Science*, 1995, vol. 269, p. 1242.
8. Antonelli, D.M. and Ying, J.Y., *Angew. Chem. Int. Ed. Engl.*, 1996, vol. 35, p. 426.
9. Fenelonov, V.B., Romannikov, V.N., and Derevyankin, A.Yu., *Micropor. Mesopor. Mater.*, 1999, vol. 28, p. 57.
10. Solovyov, L.A., Kirik, S.D., Shmakov, A.N., and Romannikov, V.N., *Micropor. Mesopor. Mater.*, 2001, vols. 44–45, p. 17.
11. Kodenev, E.G., Shmakov, A.N., Derevyankin, A.Yu., *et al.*, *J. Mol. Catal., A: Chem.*, 2000, vol. 158, p. 349.
12. Kholdeeva, O.A., Derevyankion, A.Yu., Shmakov, A.N., *et al.*, *J. Mol. Catal., A: Chem.*, 2000, vol. 158, p. 417.
13. Romannikov, V.N. and Ione, K.G., *J. Catal.*, 1994, vol. 146, p. 211.
14. Corma, A., *Chem. Rev.*, 1997, vol. 97, p. 2373.
15. Zhang, W., Froba, M., Wang, J., *et al.*, *J. Am. Chem. Soc.*, 1996, vol. 118, p. 9164.